European Journal of Pharmaceutical Sciences 173 (2022) 106163

Contents lists available at ScienceDirect

European Journal of Pharmaceutical Sciences

journal homepage: www.elsevier.com/locate/ejps

Prediction of lung exposure to anti-tubercular drugs using plasma pharmacokinetic data: Implications for dose selection

Morris Muliaditan [a], Donato Teutonico [b], Fatima Ortega-Muro [c], Santiago Ferrer [c], Oscar Della Pasqua [a,d,*]

[a] Clinical Pharmacology & Therapeutics Group, University College London, London, UK
[b] Translational Medicine and Early Development, Sanofi R&D, Chilly-Mazarin, France
[c] GlaxoSmithKline Global Health Medicines Development Campus, Tres Cantos, Madrid, Spain
[d] Clinical Pharmacology Modelling and Simulation, GlaxoSmithKline, Brentford, UK

ARTICLE INFO

Keywords:
PBPK modelling
Tuberculosis
Pharmacokinetics
Lung distribution
Rifampicin
Isoniazid
Ethambutol
Pyrazinamide

ABSTRACT

The development of novel candidate molecules for tuberculosis remains challenging, as drug distribution into the target tissue is not fully characterised in preclinical models of infection. Often antitubercular human dose selection is derived from pharmacokinetic data in plasma. Here, we explore whether whole-body physiologically-based pharmacokinetic (PBPK) modelling enables the prediction of lung exposure to anti-tubercular drugs in humans. Whole-body PBPK models were developed for rifampicin, isoniazid, pyrazinamide, and ethambutol using plasma data in mice as basis for the prediction of lung exposure. Model parameters were subsequently used to extrapolate disposition properties from mouse and determine lung:plasma ratio in humans. Model predictions were compared to biopsy data from patients. Predictions were deemed adequate if they fell within two-fold range of the observations. The concentration vs time profiles in lung were adequately predicted in mice. Isoniazid and pyrazinamide lung exposures were predicted to be comparable to plasma levels, whereas ethambutol lung exposure was predicted to be higher than in plasma. Lung:plasma ratio in humans could be reasonably predicted from preclinical data, but was highly dependent on the distribution model. This analysis showed that plasma pharmacokinetics may be used in conjunction with PBPK modelling to derive lung tissue exposure in mice and humans during early lead optimisation phase. However, the impact of uncertainty in predicted tissue exposure due to distribution should be always investigated through a sensitivity analysis when only plasma data is available. Despite these limitations, insight into lung tissue distribution represents a critical step for the dose rationale in tuberculosis patients.

1. Introduction

The dose rationale for standard of care drugs currently used as combination therapy for the treatment of tuberculosis (TB) has been established on an empirical basis, without further understanding of drug exposure in target tissues (i.e., pharmacokinetics (PK)) or the underlying pharmacokinetic-pharmacodynamic (PKPD) relationships of the active moieties. By contrast, recent efforts for the identification of novel anti-tubercular drug candidates have implemented experimental protocols, which rely primarily on PK data in plasma (Muliaditan and Della Pasqua, 2021). This approach is used to guide the dose selection of potential candidate compounds, regardless of whether drug concentrations in the systemic circulation reflect drug levels in the site of infection (lung) (Danesi et al., 2003; Kiem and Schentag, 2008; Prideaux et al., 2015a). Consequently, rapid equilibration has to be assumed between plasma and target tissue in the lung when exploring PKPD relationships. Given the heterogeneity and progression of the disease, further assumptions are also required regarding drug distribution into lesions, caseum and granuloma. Yet, to our knowledge, no systematic review of such assumptions has been performed. Understanding of target tissue exposure may be even more relevant as the prevalence of patients with co-morbidities such as HIV and SARS-CoV-2 infection appears to

Abbreviations: AUC, Area under the concentration versus time profile curve; EMB, Ethambutol; INH, Isoniazid; PBPK, Physiologically-based pharmacokinetic; PK, Pharmacokinetic; PZA, Pyrazinamide; RIF, Rifampicin; TB, Tuberculosis.

* Corresponding author at: Clinical Pharmacology & Therapeutics Group, University College London, BMA House, Tavistock Square, London WC1H 9JP, UK.
E-mail address: o.dellapasqua@ucl.ac.uk (O. Della Pasqua).

https://doi.org/10.1016/j.ejps.2022.106163
Received 27 June 2021; Received in revised form 28 December 2021; Accepted 2 March 2022
Available online 4 March 2022
0928-0987/© 2022 The Author(s). Published by Elsevier B.V. This is an open access article under the CC BY license (http://creativecommons.org/licenses/by/4.0/).

increase (Romano et al., 2021; Nardotto et al., 2022).

Serial lung biopsies cannot be collected in TB clinical trials to determine the drug exposure in human lung due to the invasive nature of the procedure. Even when such a procedure is performed, only one lung biopsy is taken per patient, yielding drug concentrations at a single time point (Prideaux et al., 2015a; Conte et al., 2000, 2001, 2002, 2004). Therefore, any attempt to describe equilibration kinetics and tissue exposure based on such sparse data needs to be interpreted with caution, especially when the sampling times are selected without taking into account the PK properties of the compound. It should be clear that following repeated dosing, drug concentrations in plasma and lung tissue will vary over time even after a system has reached steady-state (Muliaditan and Della Pasqua, 2019). Assessment of tissue to plasma ratio at a given time point cannot be considered constant.

Based on these limitations, it seems evident that serial sampling of drug concentrations from the peripheral blood will remain the standard method to study the PK properties of novel anti-tubercular drugs. As a consequence, when concentrations in plasma are higher than in lung tissue, there is a real risk that such data may lead to dose selection that results in suboptimal exposure at the site of infection (despite efficacious drug levels in plasma). By contrast, when tissue levels are higher than in plasma, there is a risk of selecting higher doses than necessary, which may result in overdosing, adverse events, and organ toxicity. Whereas information on equilibration kinetics may not be obtained during the clinical stages of development, it is clear that dose selection of anti-tubercular drugs should always take into account drug exposure at the target site, i.e., lung tissue, rather than plasma levels only.

Whole-body physiologically-based pharmacokinetic (PBPK) modelling is a tool that is often applied in drug development to predict tissue concentrations from plasma data (Sadiq et al., 2017). In this approach, the physicochemical properties of the compound of interest can be combined with available anatomical and physiological knowledge (e.g. haemodynamics) to characterise drug distribution and tissue exposure. To that purpose, various distribution models have been identified that reflect drug disposition properties, allowing prediction of the drug concentration across different tissues and organs (Kuepfer et al., 2016). Consequently, the accuracy of such predictions depends on the selection of the correct distribution model as well as knowledge of the mechanisms of distribution and elimination (Carrara et al., 2020).

The development of a suitable whole-body PBPK model requires experimental data along with parameters that describe organ blood blow and haemodynamics. Ideally, it can be implemented in preclinical species and used to scale up and predict tissue exposure in humans. Among other things, serial sampling of tissue concentrations at various dose levels should be performed in preclinical protocols for the evaluation of PK to support the selection of the best distribution model during the PBPK model building (Kuepfer et al., 2016). The *in vivo* PBPK model can be subsequently harnessed to better inform dose selection for first-time-in-human studies, prior to the start of the actual clinical trial. Unfortunately, the use of destructive sampling may still pose a major limitation for serial collection of tissue concentrations during PK studies in animals, especially when more than one drug candidate and multiple dose levels need to be evaluated.

The objective of the current investigation is therefore to explore whether the use of whole-body PBPK modelling in conjunction with PK data in plasma is predictive of lung tissue exposures of anti-tubercular drugs in mice and humans. The approach proposed here specifically aims to mimic data availability at the early lead optimisation phase, during which usually only plasma PK after single doses is collected in mice. First-line anti-tubercular drugs rifampicin (RIF), isoniazid (INH), pyrazinamide (PZA) and ethambutol (EMB) were selected as paradigm compounds. We anticipate that our findings may support further optimisation of experimental protocols for novel candidate molecules for the treatment of TB.

2. Materials and methods

2.1. In vivo pharmacokinetics

PK studies were performed using C57BL/6J female mice (weight: 18–21 g). An overview of dose groups and sampling scheme used for the characterisation of plasma and lung tissue concentrations is shown in **Table 1.** All mice received treatment in the fed state. All drugs were administered as a single dose intravenously (IV) or by oral gavage (PO). RIF was administered in 20% Encapsin aqueous solution; INH was administered in Milli Q water; EMB and PZA were administered in saline (IV) and in 1% methyl-cellulose (PO). Blood samples ($n = 3$ mice per sampling time per compound) were collected by cardiac puncture (following euthanasia by CO_2) at 0.08, 0.25, 0.5, 0.75 1, 1.5, 2, 3, 4, 8 and 24 (EMB only) hours post dose for RIF, INH and EMB. Lungs ($n = 3$ mice per sampling time per compound) were additionally removed based on the same sampling scheme. For PZA, blood samples ($n = 3$ mice per sampling time per compound) were collected by cardiac puncture (following euthanasia by CO_2) at 0.08, 0.25, 0.5, 0.75 1, 1.5, 2, 3, 4 and 8 h post IV dose and from individual mice ($n = 3$ per dose) via the lateral tail vein at 0.25, 0.5, 0.75 1, 2, 4, 6, 8 and 24 h post PO dose. Drug concentrations in blood, plasma and lungs were determined by LC-MS/MS. The lower limit of quantification is from 5 to 20 ng/ml for RIF, INH and EMB to 500 ng/ml for PZA. Given that only whole blood concentrations were available for PZA, plasma concentrations were converted from blood concentrations using a blood/plasma (B/P) ratio of 0.79 (internal unpublished data). All experimental protocols were ethically reviewed and carried out in accordance with European Directive 2010/63/EU and the GSK Policy on the Care, Welfare and Treatment of Animals.

2.2. Conversion of tissue levels to plasma concentration unit

In order to compare drug concentrations in lung to plasma using the same unit (μg ml^{-1}), reported tissue levels (μg g^{-1}) were converted to μg ml^{-1} using the following Eq. (1):

$$DV_{lung\ (\mu g/mL)} = \frac{DV_{lung\ (\mu g/g)} \cdot WT_{lung}}{V_{lung}} \quad (1)$$

where DV is the drug concentration, WT_{lung} the weight of lung in mice (0.14 g; internal data) or human (830 g) (Molina and DiMaio, 2012) and V_{lung} the volume of lung in mice (0.1 ml) or human (930 ml) (Lippert et al., 2019).

2.3. PBPK model building in mice

2.3.1. General model building strategy and initial preparations prior to estimation step

A whole-body PBPK model as implemented in PK-Sim (Lippert et al., 2019) (**Fig. 1**) was developed for each drug using the available mouse PK data. *In vivo* data was integrated with relevant *in vitro* and physiological data. For the development of whole-body PBPK models, it was

Table 1
Overview of the doses of rifampicin, isoniazid, pyrazinamide and ethambutol for which plasma and tissue samples were collected. Drugs were administered orally, unless stated otherwise.

	Doses for which drug concentrations were available (mg kg^{-1})	
Compound	Plasma	Lung tissue
Rifampicin	1, 3, 10, 12 (IV), 30, 100	10, 100
Isoniazid	0.1, 0.5, 1, 5, 10 (IV), 25	0.5, 5, 25
Ethambutol	10, 16 (IV), 30, 100, 300, 1000	10, 100, 1000
Pyrazinamide[1]	15, 25, 25 (IV), 50, 150, 400, 1000	150[2]

IV = intravenous; (1) whole blood concentrations; (2) extracted from (Irwin et al., 2016).

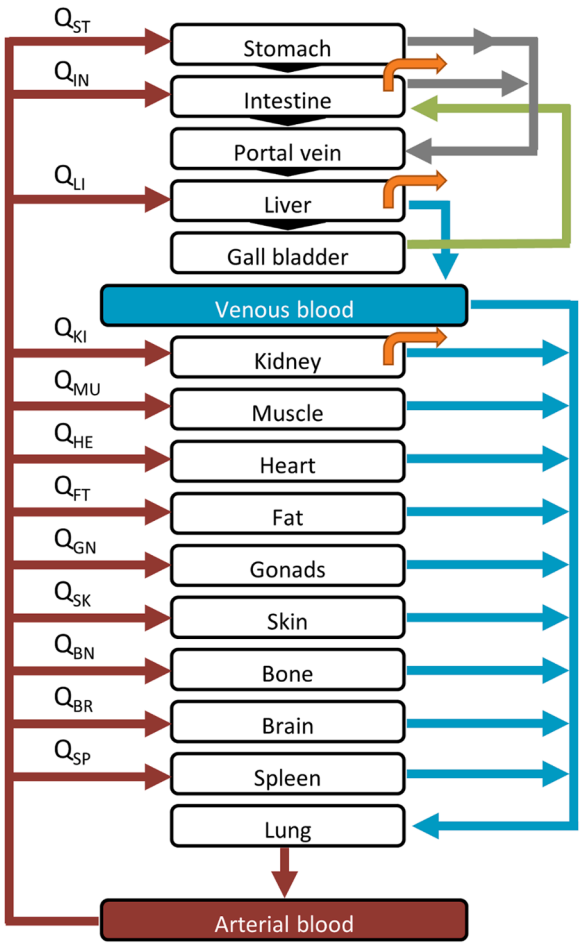

Fig. 1. Schematic diagram of the whole-body PBPK model as embedded in PK-Sim software. Arrows depict the organ blood flows (Q). Orange arrows indicate possible elimination pathways that can be included in the model (For interpretation of the references to color in this figure legend, the reader is referred to the web version of this article.).

assumed that plasma concentrations corresponded to levels in venous blood. An outline of the general model building strategy is presented in Fig. 2 as previously outlined (Kuepfer et al., 2016).

Due to limitations in the experimental protocols, complementary PK information (i.e., plasma and lung concentrations) were digitized from the published literature and used in conjunction with the available data sets. Serum concentrations following single IV administration of 10 mg/kg RIF in male CD1 mice (20–27 g) were included to support estimation of the disposition parameters in the RIF PBPK model. Details of the experimental protocol can be found elsewhere (Bruzzese et al., 2000). In addition, as *in vivo* lung tissue concentrations of PZA were not collected in the initial experiments, predicted lung tissue/plasma ratio was validated against published whole lung tissue/plasma ratio measured in female BALB/c mice following single administration of 150 mg/kg PZA via oral gavage. We have assumed that PZA disposition was not significantly different between BALB/c and C57BL/6J mice. Full details of the experiment can be found elsewhere (Irwin et al., 2016). Plasma and lung concentrations were digitized from the publication and were added to the data set for the PBPK model building.

As the aim of this analysis was to mimic early preclinical development and no data were collected regarding the fraction of drug excreted in the bile and urine, it was not possible to implement a more sophisticated PBPK model, in which the contribution of different routes of elimination can be described separately. Instead, we have decided to apply a simplified model building strategy, in which PBPK modelling is envisaged to support drug candidate selection by predicting which compounds will most likely yield favourable lung tissue distribution.

To accelerate the model building process without compromising the quality of the analysis, a more practical PBPK modelling approach was proposed, which can be implemented using current experimental protocols. Consequently, a general liver clearance and renal excretion route were used instead. More details are provided in the next section. System-specific (physiological) parameters were fixed to the default value in the PK-Sim software, while for each drug a prespecified set of drug-specific parameters were either estimated from the mouse plasma PK data or fixed to published literature values (Fig. 2).

Table 2 provides an overview of the drug-specific parameters (i.e. physicochemical properties, protein binding) and the values to which these parameters were fixed. Mouse protein binding was assumed to be similar between mouse strains (C57BL/6J, BALB/c, CD1) and fixed to experimental values obtained in our labs. Finally, as *in vivo* doses were originally reported in mg/kg, the actual dose in mg was calculated assuming that each mouse weighed either 20 g (C57BL/6J and BALB/c) or 25 g (CD1).

2.3.2. Estimation of the remaining drug-specific parameters in the PBPK model

The Monte-Carlo algorithm in the PK-Sim software was used to estimate the relevant PBPK parameters. As described previously, the proposed approach for model building consisted in the use of IV PK data to estimate the lipophilicity and characterise the distribution properties of the drugs. Estimation was performed using all five distribution models, as implemented in the PK-Sim software. Given that lung tissue concentrations were considered for validation purposes only (rather than informing selection of the best distribution model), the goodness-of-fit for the predicted plasma concentration vs. time profile was evaluated for each distribution model. The best fit was used as criteria for selection of the distribution model. Details on the difference between each distribution model (Berezhkovskiy, PK-Sim, Poulin and Theil, Rodgers and Rowland, Schmitt) have been published elsewhere (Kuepfer et al., 2016). The lipophilicity estimates for each compound were then fixed and the model re-run with inclusion of the oral PK data. During this step, the transcellular intestinal permeability was estimated to describe the absorption processes of the drugs. Drug metabolism was described with first-order total hepatic clearance, with the exception of PZA. For PZA, an initial evaluation of the oral data suggested nonlinear PK. However, as the data collected after IV administration was based on a single dose level, lipophilicity estimates were obtained assuming first-order elimination. Saturation kinetics was tested subsequently with a Michaelis-Menten process after inclusion of the data from oral administration. For the purposes of our analysis, it was assumed that metabolic activity was limited to the liver. Renal excretion was accounted for in the model by including glomerular filtration rate (GFR), with a GFR fraction fixed to 1. This implies the assumption that no active processes (i.e. tubular secretion or re-absorption) were involved in the excretion of the drugs of interest.

2.4. Assessment of the PBPK model performance in mice

Initially, goodness-of-fit plots were used to assess model performance. Once fitting of plasma concentration vs. time profiles was deemed adequate for each distribution model, an attempt was made to evaluate the predictive performance of the model to describe drug concentrations in lung tissue. The ratio between predicted and observed lung exposure was used as a diagnostic criterion for model performance. Lung:plasma ratio and lung tissue exposure (measured by the area under the time versus concentration profile, $AUC_{0\text{-}\tau}$) were selected as parameters of interest. The trapezoidal rule was used to calculate $AUC_{0\text{-}\tau}$ in the entire analysis. Model performance was deemed adequate if the concentration vs. time profiles in lung tissue were adequately described and differences between predicted and observed lung $AUC_{0\text{-}\tau}$ and lung:

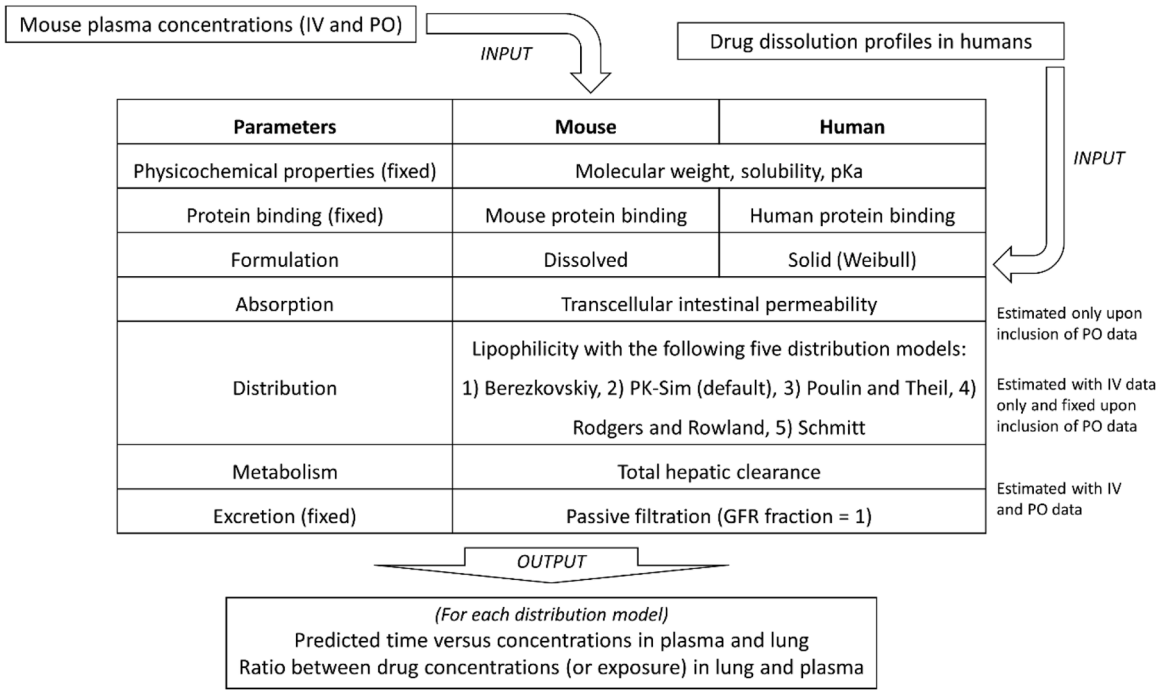

Fig. 2. Schematic overview of the PBPK model building strategy applied to the current analysis. Parameter estimates describing the physicochemical properties and plasma protein binding of each drug were fixed to the published literature values. Mouse plasma concentrations were used for the initial PBPK model, in which parameters related to absorption, distribution and metabolism were estimated in a stepwise manner, as indicated by the diagram arrows. For the extrapolation from mice to humans, most model parameters remained the same, except for formulation and protein binding. All system parameters (e.g. organ blood flow) were also scaled to human values. IV = intravenous; PO = oral. GFR = glomerular filtration rate.

Table 2
Drug-specific parameters which were fixed during whole-body PBPK model building.

Parameters	Rifampicin	Isoniazid	Ethambutol	Pyrazinamide
Molecular weight (g mol^{-1}) (Lakshminarayana et al., 2015)	822.96	137.14	204.31	123.12
Fraction unbound (%)[1]				
Mouse	2.9	40	83	59
Human	7.8	52	85	72
pKa	7.9 (base), 1.7 (acid) (TB Alliance 2008a)	1.82 (base)[2]	6.25 (base), 9.35 (base) (TB Alliance, 2008b)	0 (base)[3]
Solubility (mg ml^{-1}, pH 7.4) (Lakshminarayana et al., 2015)	1.79	4.93	7.58[2]	150[2]

[1] *Data generated by GlaxoSmithKline;*
[2] *DrugBank* (DrugBank, 2020a–2020c) *(experimental);*
[3] *PK-Sim did not allow negative value as input for pKa (-0.5 as reported in Drugbank). Parameter was hence fixed to zero as it is closest to literature value.*

plasma ratio were not larger than 2 fold. Such a criterion is commonly used to assess the predictive performance of PBPK models (De Buck et al., 2007; Poulin et al., 2011).

2.5. Translation and prediction of drug exposure in tuberculosis patients

2.5.1. Initial preparations prior to prediction of drug exposure in humans

Interspecies differences in physiology were accounted for in PK-Sim by switching the physiological parameters of the model from "mice" to "humans". This step automatically replaces the anatomy (e.g. organ volumes) and physiology (e.g. blood flow rates) of the subjects included in the PK simulations. A comparison of the relevant physiological parameters in humans and mice is shown in **Supplementary Materials (Table S1)**. The remaining PBPK model components and corresponding drug-specific parameters were kept to the values that were previously estimated using mouse data, with the exception of protein binding (**Table 2**) and drug formulation, which changed from oral solution to tablets.

Since drugs were administered in humans as solid dosage forms, a dissolution function had to be included in the human PBPK model to describe the dissolution process of the tablets. An overview of the model fitting and estimated Weibull parameters that were used to describe the dissolution profiles of RIF, INH, PZA and EMB in humans is provided in the **Supplementary Materials (Fig. S1)**.

2.5.2. Lung biopsy data in tuberculosis patients

The predictive performance of the PBPK models for RIF, INH and PZA in humans was assessed using lung biopsy data from the published literature. Blood samples and tissue biopsy were collected from 15 Asian multidrug resistant (MDR)-TB patients who underwent lung resection surgery (**Fig. S2**) (Prideaux et al., 2015a). In this study, all patients concomitantly received a single dose of INH (300 mg), RIF (600 mg; 450 mg when patient weighed <50 kg), 1500 mg PZA and 400 mg moxifloxacin (MXF). No drug-drug interaction between these drugs was anticipated. All drugs were administered at 2, 4, 8, 12 or 24 h prior to surgery. Some patients were already at state levels for INH ($N = 3$; 20%) and/or PZA ($N = 4$; 27%) as they had received these drugs as part of their background drug regimen for several weeks or months before surgery. Further details regarding the original study design, as well as the processing and analysis of the blood samples and lung biopsies to derive the plasma and tissue concentrations can be found in the original publication (Prideaux et al., 2015a). Unfortunately, no information could be found in the literature regarding the lung tissue exposure of EMB in humans; therefore, only predicted EMB concentrations in lung

were derived.

2.5.3. Virtual population and study design for the assessment of the predictive performance of the PBPK model in tuberculosis patients

To mimic the population in the reference lung biopsy study, a virtual Asian population consisting of 1500 subjects (60% male) was first simulated using the baseline demographic characteristics (e.g. median and range values) from the study by Prideaux et al. (2015a) and the PK-Sim Asian population database (Tanaka and Kawamura, 1996). Given that most observed INH and PZA concentrations in the study by Prideaux et al. were derived following single dose administration, concentration vs. time profiles in plasma and lung tissue were simulated following a single dose administration of 600 mg RIF, 300 mg INH, 1100 mg EMB and 1500 mg PZA to mimic the original study design. We assumed that EMB tablets were administered in its hydrochloride formulation (EMB-HCL). The actual dose of EMB was calculated as the fraction relative to EMB-HCL, which was 74% or equivalent to 814 mg EMB.

2.6. Evaluation of the predicted lung tissue exposure in tuberculosis patients

Given the sparse sampling schedule used in the Asian patient population (**Fig. S2**), $AUC_{0\text{-}\tau}$ in plasma and lung tissue could not be calculated. Instead, simulated concentration profiles (in plasma and lung tissue) were superimposed to the observed data using the selected distribution model. These profiles take into account the contribution of demographic covariates, with baseline characteristics matching those of the original population in Prideaux et al. (2015a) (**Fig. S3**). Median age, weight and body mass index (BMI) of the virtual population were respectively 41 years (range, 23–59), 58.6 kg (range, 49.8–83.6) and 22 kg m^{-2} (range, 17.4–29.3). Albeit limited, the predictive performance was subsequently assessed by comparing predicted and observed profiles. The median observed ratio of lung:plasma concentrations for each patient (calculated around the time point in which the lung biopsy was taken) was also compared to the predicted ratio between $AUC_{0\text{–}24}$ in lung tissue and plasma as a secondary validation step.

2.7. Software

PBPK models were built using PK-Sim 6.2, which is currently part of the Open Systems Pharmacology software package (Lippert et al., 2019). WebPlotDigitizer was used to extract data from figures in the publications (Rohatgi, 2020). All other steps relative to data preparation, formatting and graphical analysis were performed in R v3.2.5 (R Core Team, 2020). No formal statistical hypothesis testing other than the pre-defined diagnostic criteria was used for the evaluation of the predictive performance of the models.

3. Results

3.1. In vivo whole-body PBPK model building

The final PBPK parameter estimates are presented in **Supplementary Materials (Table S2)**. As shown in **Fig. 3**, plasma concentrations of RIF, INH, PZA and EMB in mice were adequately described by the PBPK model. No major differences were found between the five distribution models with regard to the predicted plasma concentration profiles. These results showed that the decision on selecting the best distribution model for predicting tissue concentrations cannot be made based on plasma concentrations alone. As such, predicted tissue concentrations of each distribution model will be shown in subsequent sections.

Estimated logP values were close to the experimental values for RIF and INH, but larger differences were observed for PZA and EMB. The implications of these differences were assessed during the external validation of the calibrated distribution parameters (e.g. lipophilicity) based on IV plasma data, which are shown in the next section using lung tissue data.

3.2. Model-predicted lung tissue concentration vs. time profiles in mice

Concentration vs time profiles of RIF, PZA and INH in lung tissue

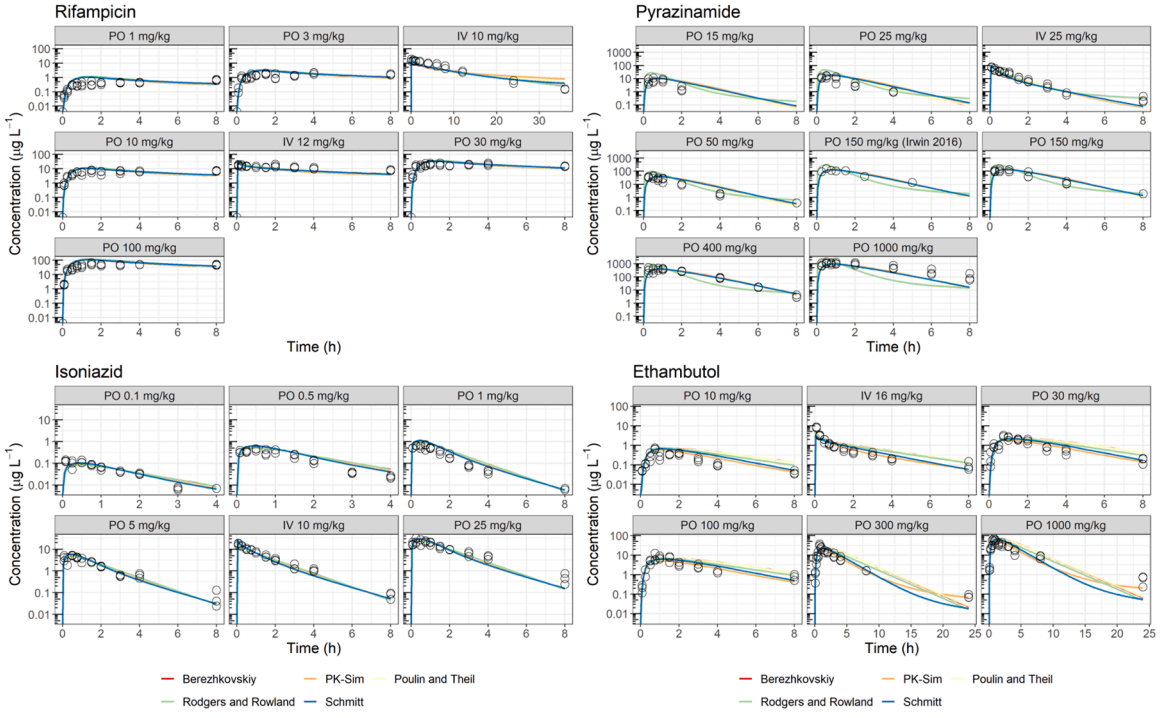

Fig. 3. PBPK model predicted plasma concentration vs. time profiles of rifampicin, isoniazid, pyrazinamide, and ethambutol in mice ($N = 3$ per time point). Open circles denote the observed data while the different solid lines represent the predicted profile for each distribution model as implemented in PK-Sim.

were in general adequately predicted. Consequent to the similar predictions obtained by the different distribution models for plasma concentrations (Fig. 4), no decision could be made on which distribution model should be selected for the prediction of lung tissue exposure in humans. In contrast, major discrepancies were observed between the distribution models for the predicted EMB lung concentrations, with the Berezhkovskiy and Poulin and Theil distribution models performing best (Fig. 4). Model-predicted $AUC_{0\text{-}\tau}$ was derived from the predicted concentration versus time profiles to describe total exposure in lung and plasma of mice (**Table S3**). The predicted median $AUC_{0\text{-}\tau}$ in the mice lung tissue fell in general within the two-fold error margin of the observations, with Berezhkovskiy and Poulin and Theil distribution models demonstrating the best overall *in vivo* predictive performance (Fig. 5). An overview of model-predicted and observed lung:plasma ratio in mice is summarised in Table 3.

The lung:plasma $AUC_{0\text{-}\tau}$ ratio of RIF in mice was dose dependent. This resulted in observed RIF lung exposure at 10 mg kg^{-1} to be lower than the values observed in plasma (0.48-fold). By contrast, lung exposure at 100 mg kg^{-1} was 1.26 fold higher than plasma. Despite evidence that these values fall within the predicted range (0.45–1.3), the PBPK model could not predict dose-dependent tissue equilibration. Similarly, our data showed that EMB exposure in lung tissue was consistently higher as compared to values in plasma, with lung:plasma $AUC_{0\text{-}\tau}$ ratio decreasing (from 11.8 to 6.34) with doses increasing from 10 to 1000 mg kg^{-1}. Model-predicted ratio was much wider as compared to RIF, ranging from 1.54 (PK-Sim distribution model) to 17.5 (Schmitt distribution model). Observed INH lung:plasma $AUC_{0\text{-}\tau}$ ratio was comparable across all doses evaluated (i.e., approximately 1). These results were similar to model-predicted values (0.49–0.66). A similar pattern was observed for PZA, for which a lung : plasma $AUC_{0\text{-}\tau}$ ratio of 1.21 was observed, while model-predictions ranged between 0.56 and 0.71.

3.3. Model-predicted lung tissue concentrations vs. time profiles in tuberculosis patients

Predicted concentration vs. time profiles in human plasma and lung tissue are shown in Fig. 6. Predicted lung tissue profiles in humans varied more significantly between the distribution models as compared to the predicted profiles in mice. None of the distribution models was able to predict both plasma and lung tissue concentrations in patients adequately (Fig. 6).

RIF lung tissue concentrations (but not plasma profiles) were best predicted with PK-Sim and Poulin and Theil distribution models. By contrast, the Rodgers and Rowland distribution model yielded better predictions for RIF plasma concentrations but under-predicted RIF elimination from lung tissues. Reasonable predictions of INH plasma concentrations were obtained with the Berezhkovskiy and Poulin and Theil distribution models, but all of them appeared to overpredict INH concentrations in lung tissue. PZA lung profiles were best described by the Rodgers and Rowland distribution model, but PZA elimination from plasma was over-predicted by all distribution models (Fig. 6).

Predicted $AUC_{0\text{-}\tau}$ estimates were derived from the predicted concentration vs. time profiles to describe total exposure in the lung and plasma of TB patients (**Table S4**). An overview of predicted and observed lung:plasma ratio in the TB patients is summarised in Table 4.

The predicted lung:plasma $AUC_{0\text{-}\tau}$ ratio of INH and PZA were comparable across distribution models (i.e. 0.57–0.75 and 0.53–0.76, respectively). On the other hand, our findings show that the predicted lung:plasma $AUC_{0\text{-}\tau}$ ratio of RIF was more sensitive to the choice of distribution model, with the Berezhkovskiy and Rodgers and Rowland distribution models yielding respectively the lowest (0.66) and highest lung:plasma $AUC_{0\text{-}\tau}$ ratio (2.09). The widest prediction range was observed for EMB (1.08–19.9).

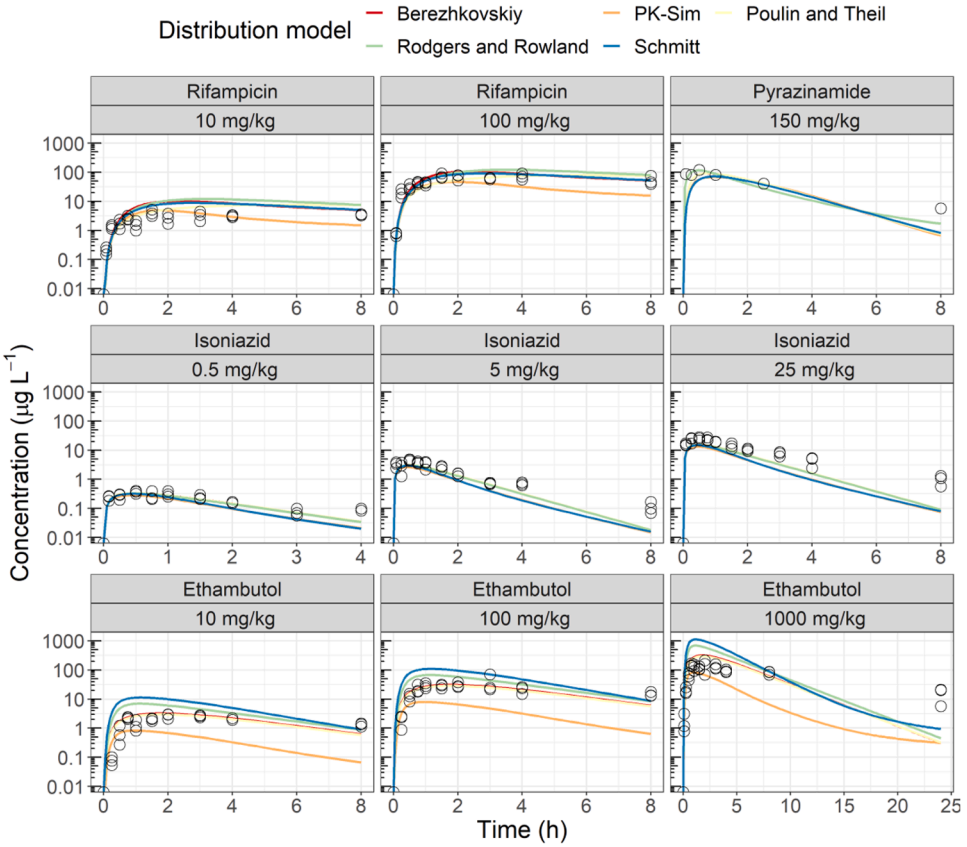

Fig. 4. PBPK model predicted concentration vs. time profiles of rifampicin, isoniazid, pyrazinamide, and ethambutol in mice lung tissue ($N = 3$ per time point). Predictions are based on a model built on plasma concentrations alone. Solid lines represent the predicted profile for each distribution model as implemented in PK-Sim, whilst open circles depict the observed concentrations. In contrast to ethambutol, no differences in the predictive performance of the distribution models were observed for rifampicin, isoniazid, and pyrazinamide.

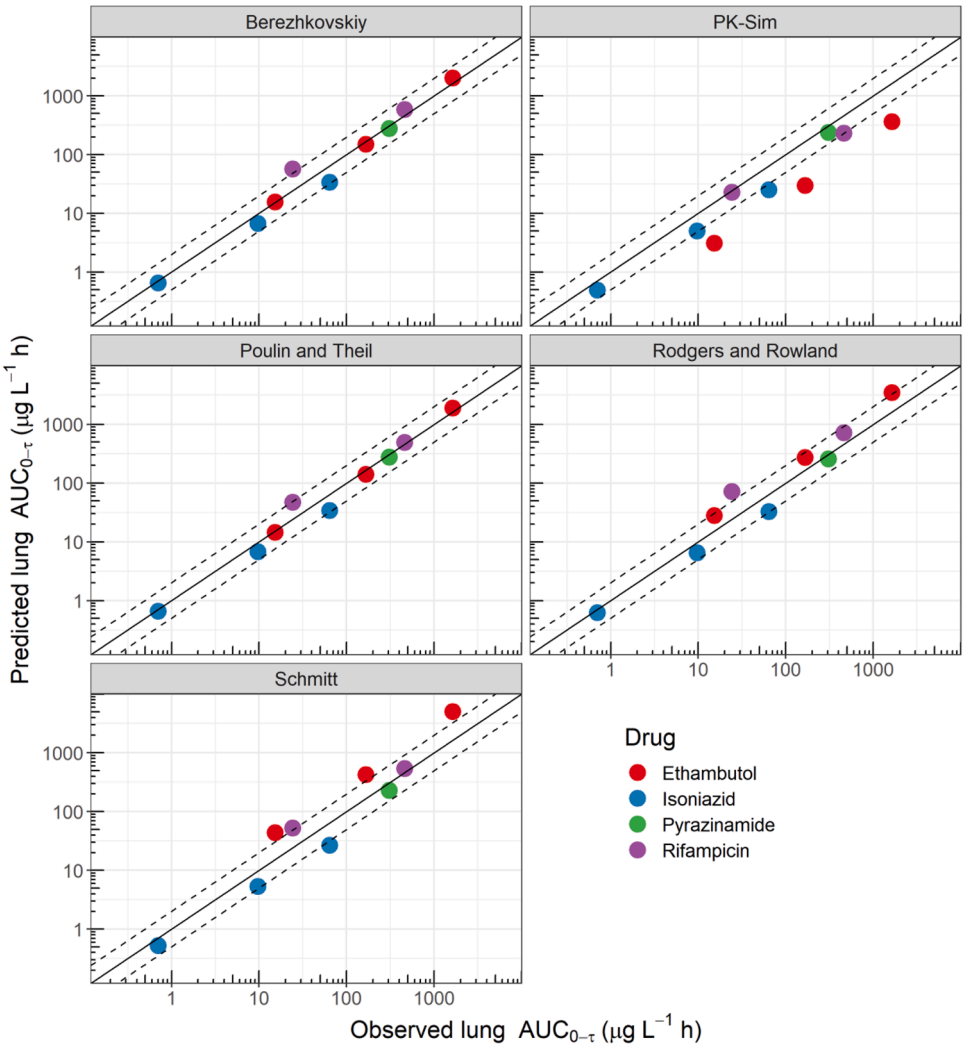

Fig. 5. Predicted versus observed $AUC_{0-\tau}$ of rifampicin, isoniazid, pyrazinamide, and ethambutol in mice lung tissue for each distribution model in PK-Sim. Solid line depicts the identity line, whilst dashed lines represent the two-fold range relative to the observed data. AUC = area under the concentration vs. time curve. Predictions were derived by the PBPK model built on plasma concentration data alone.

Table 3
Overview of the PBPK model predicted median lung:plasma $AUC_{0-\tau}$ ratio in mice as compared to the observed values ($N = 3$ per time point).

Drug	Dose (mg/kg)	Observed lung:plasma $AUC_{0-\tau}$ ratio	Predicted lung:plasma $AUC_{0-\tau}$ ratio					
			Range	Berezhkovskiy	PK-Sim	Poulin and Theil	Rodgers and Rowland	Schmitt
Mice								
Rifampicin	10	0.48	0.45–1.3	1.11	0.45	0.94	1.3	1.03
	100	1.26						
Isoniazid	0.5	0.97	0.49–0.66	0.66	0.49	0.66	0.64	0.51
	5	0.98						
	25	1.09						
Pyrazinamide	150	1.21	0.56–0.71	0.71	0.61	0.71	0.56	0.58
Ethambutol	10	11.8	1.54–17.5	4.8	1.54	4.56	9.43	17.5
	100	8.31						
	1000	6.34						

AUC = area under the concentration vs. time curve.

4. Discussion

While PBPK models have been previously developed for the evaluation of anti-tubercular drugs (Cordes et al., 2016; Gaohua et al., 2015; Lyons et al., 2013; Reisfeld et al., 2012; Zurlinden et al., 2016), these publications have primarily focused on model building and data fitting, without emphasis on the quantitative and translational pharmacology aspects, which underpin the selection and ranking of compounds in early drug development (Della Pasqua, 2013; Muliaditan et al., 2017). In fact, none of the publications has explored whether PBPK models can be used *a priori* to predict lung concentrations in mouse and humans based on *in vivo* plasma concentrations alone. As such, to our knowledge, this is the first investigation to date which assesses the performance of PBPK modelling for the prediction of lung tissue concentrations in animals and

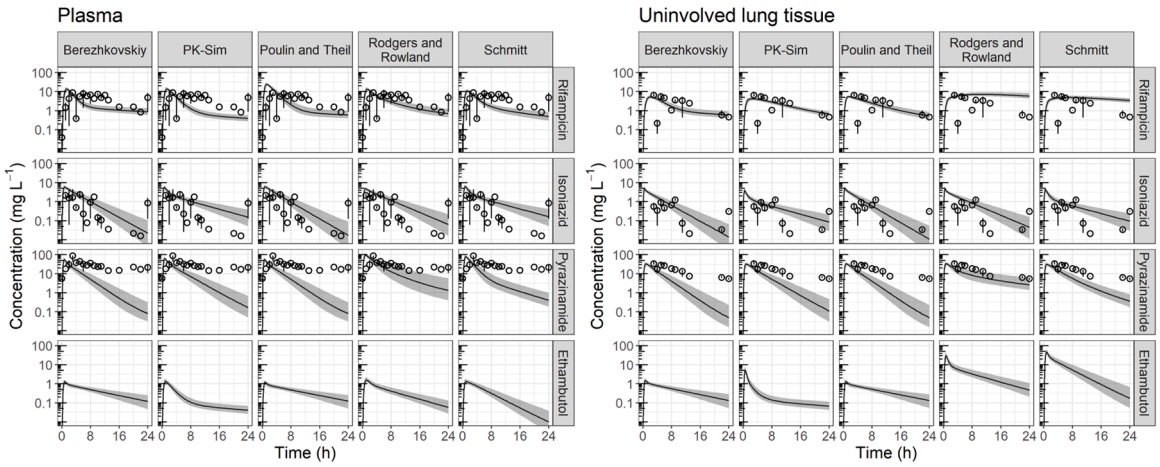

Fig. 6. PBPK model predicted concentration vs. time profiles ($n = 1500$) of rifampicin, isoniazid and pyrazinamide in plasma and healthy lung tissue in tuberculosis patients. Solid lines and shaded area represent model predictions and 90% confidence intervals. Open circles and vertical lines depict the median observed concentrations and the corresponding 90% confidence interval at each time point. Observed concentrations in lung tissue (each open circle = 1 patient) were obtained from Prideaux et al. (2015a). These results show that a PBPK model based on *in vivo* plasma concentrations alone does not accurately predict lung tissue concentrations in tuberculosis patients.

Table 4
Overview of PBPK predicted lung:plasma $AUC_{0\text{-}\tau}$ ratio in tuberculosis patients ($n = 1500$) as compared to observed values ($N = 15$) (Prideaux et al., 2015a). AUC = area under the time versus concentration curve.

Drug	Dose (mg)	Observed lung:plasma concentrations ratio (median, range)[1]	PBPK model predicted lung:plasma AUC_{0-24} ratio				
			Range	Berezhkovskiy	PK-Sim	Poulin and Theil	Rodgers and Rowland	Schmitt
Rifampicin	600	0.46 (0.04–1.15)	0.53–2.09	0.66	0.91	0.53	2.09	1.93
Isoniazid	300	0.42 (0.26–2.69)	0.57–0.75	0.67	0.57	0.67	0.75	0.6
Pyrazinamide	1500	0.47 (0.21–1.06)	0.53–0.76	0.76	0.69	0.76	0.53	0.65
Ethambutol	1100	N/A	1.08–19.9	1.12	1.67	1.08	9.35	19.9

[1] *Lung:plasma AUC_{0-24} could not be calculated due to sparse data. As such, the individual median ratio of the lung and plasma concentrations was initially calculated. We subsequently presented the median and range values of the calculated individual lung:plasma ratio; N/A = not available.*

humans.

In line with evolving trends regarding the use of PBPK modelling for the characterisation of drug-drug interactions and scaling of PK from adults to special populations (Abouir et al., 2021, Jones et al., 2013, Bellanti and Della Pasqua, 2011), our analysis shows that PBPK models based on plasma data across a relevant dose range are predictive of lung tissue exposure in mice. Interestingly, these same models were found to be predictive for lung:plasma ratios in humans. Whilst lung:plasma ratios for anti-tubercular drugs were similar to observed values, these predictions were associated with considerable uncertainty in parameter estimates, which is mostly due to the identification of the correct distribution model. These results suggest that PBPK models based on mouse plasma data may only be useful to predict the tissue distribution properties of the drug in mice, but more data (e.g. PK data from different animal species) is required for the prediction of lung tissue exposure profile in humans.

It should also be clear that the current implementation of PBPK models does not account for active processes in drug distribution, given that such data are often unavailable or unknown in early drug development. In addition, knowledge of the ADME properties of a compound may be limited at the time of candidate selection, in particular, the role of renal processes in the overall elimination of a compound from the body. The implications of such uncertainty is exemplified by the findings for EMB, which is excreted renally by passive and active mechanisms (Lee et al., 1977; Lee et al., 1980), but for which no urine data was available in mice or humans. In fact, previous research has shown that model misspecification and poor predictions are more frequent when multiple elimination processes or active processes are involved (Jones et al., 2006).

4.1. *Data requirement for the use of PBPK modelling as a tool for the prediction of drug concentrations in human lung tissue*

Overall, these findings indicate that the development of PBPK models based on mouse plasma data alone is insufficient to predict *a priori* human PK (whether in plasma or lung tissue). On the other hand, implementation of a typical PBPK modelling approach based on the use of PK data from multiple species in conjunction with more *in vitro* data is not feasible due to the lack of suitable data, as would have been the case during early lead optimisation in a real-life setting. Furthermore, preclinical protocols for the evaluation of pharmacokinetic data often overlook the contribution of the underlying disease to changes in tissue perfusion and composition, which may differ significantly across species.

Nevertheless, this investigation has demonstrated that it is difficult to identify the correct distribution characteristics of the compound using only plasma data, which consequently leads to uncertainty and bias in drug concentrations at the target tissue. As can be seen from the comparative analysis of data from four different drugs, model-predictions depend on the selection of the appropriate distribution model as well as on the quality of the blood sampling scheme (Huang and Isoherranen, 2020). These requirements cannot be overlooked when PBPK models are used to support the prediction of efficacious human exposure and therapeutic dose range.

If only plasma concentrations are available, it should be noted that it may not be possible to identify the distribution model that best describes tissue exposure profiles. Consequently, biased predictions of tissue concentrations can be anticipated if the wrong distribution model is used. Using RIF as example, the distribution model with the best predictive performance for human plasma exposure (Rodgers and Rowland) in fact did not yield the best performance for lung exposure (PK-Sim/Poulin and Theil distribution models). Since predicted tissue exposure is greatly determined by the distribution model, the impact of uncertainty due to distribution should be characterised through a sensitivity analysis. This can be achieved, at least partially, by exploring the variability of the predicted lung concentrations using the different distribution models, as was done in current analysis.

Moreover, lung tissue distribution of EMB, which is charged at physiological pH, did not appear to be better described by distribution models that take into account drugs dissociation, such as the Rodgers & Rowland or Schmitt models. This supports the best-practice that distribution models should be selected based on fitting of the available data without a priori assumptions (Kuepfer et al., 2016). It should be acknowledged, however, that the distribution model was selected based on tissue data from a single species, which reflects the experimental package available during the lead optimisation phase. The use of data from different animal species would provide a valid basis for the selection of the appropriate distribution model. However, an important limitation remains to be addressed, namely that preclinical protocols for the evaluation of pharmacokinetic data often overlook the contribution of the underlying disease to changes in tissue perfusion and composition, which may differ significantly across species.

4.2. Limitations

We acknowledge that we have not exhausted all options that in traditional settings would have been explored to optimise the PBPK models (i.e. inclusion of *in vitro* data and PK data from other species such as rat, monkey, or dog to inform IVIVC) prior to human PK predictions. Such traditional data-driven PBPK modelling approach was beyond the scope of our investigation, as this exercise attempted to provide insight into the predictive performance of a simplified PBPK model building strategy based only on plasma PK data from mouse to be implemented during lead optimisation. At this stage of drug development, *in vitro* data (e.g., Caco-2 permeability, microsomal clearance) and PK in multiple (non-rodent) species have yet to be generated. On the other hand, whilst the use of *in vitro* human data (such as hepatocyte or microsomal clearance or Caco-2 permeability) and PK data from multiple species could have improved the predictions, such an evaluation would only be feasible at a much later stage of development.

Despite such limited input data, we have shown that there may be value in implementing PBPK modelling as a tool for a more robust ranking of novel compounds based on the predicted lung:plasma ratio in humans, than simply relying on observed drug levels in tissue homogenate. However, it should be noted that prediction of the drug permeability and distribution into lung granulomas from animal models may be quite challenging, as most experimental models of infection show pathophysiological characteristics that differ from the clinical presentation of the disease in humans. We also acknowledge that a major limitation of the approach proposed here is the fact that lung tissue concentrations are derived from organ homogenates, which may not be a suitable surrogate for concentrations at the site of infection (Kjellsson et al., 2012). It should be emphasised that only a few animal infection models share the complex pathological hallmarks (e.g. lesion formation) observed in TB patients (Lenaerts et al., 2015). Even then, disease features in these animal models may still remain much less differentiated than human lesions (Kjellsson et al., 2012). In addition, one should not underestimate the technical difficulties for the bioanalysis of drug concentrations at the various lesion compartments. There may be only a small number of specialised labs worldwide where such measurements can be performed using alternative methods, such as matrix-assisted laser desorption ionisation mass spectrometry imaging (Prideaux et al., 2015b). Finally, one needs to take into account inter-individual variability in lung:plasma exposure ratio in humans, which cannot be predicted *a priori* from any preclinical data (Muliaditan and Della Pasqua, 2019). Indeed, adequate matching of individual human lung biopsy concentrations in this analysis has been hindered by the considerable between-subject variability in the data.

5. Conclusions

Regardless of these limitations, our analysis suggests that the use of PBPK models in conjunction with single dose PK data across a relevant dose range in mice could be informative for TB drug developers as an exploratory tool during early lead optimisation. Integration of knowledge regarding tissue distribution properties of novel drug candidates can be pivotal for the characterisation of the antibacterial activity *in vivo*. Moreover, such information may facilitate the ranking of compounds for progression into clinical development. PBPK model refinement should therefore be considered as a continuous iterative process, during which additional *in vitro* and *in vivo* data is incorporated into the model to support human dose predictions prior to first-time-in-human studies.

In summary, our investigation shows that the accuracy and precision of model predictions for lung tissue exposure in humans depends on the choice of the distribution model, which ideally is informed by PK data from multiple animal species. However, further understanding of drug disposition processes, including the effect of disease-related changes in tissue perfusion and composition is required to ensure accurate extrapolation of parameters describing drug exposure at the site of infection in TB patients.

CRediT authorship contribution statement

Morris Muliaditan: Conceptualization, Formal analysis, Writing – original draft, Writing – review & editing. **Donato Teutonico:** Conceptualization, Methodology, Writing – review & editing. **Fatima Ortega-Muro:** Investigation, Data curation, Writing – review & editing. **Santiago Ferrer:** Investigation, Data curation, Writing – review & editing. **Oscar Della Pasqua:** Conceptualization, Writing – original draft, Writing – review & editing.

Declaration of Competing Interest

The authors declare no conflict of interest.

Ethical approval

Not applicable.

Funding information

No funding was received for this study.

Supplementary materials

Supplementary material associated with this article can be found, in the online version, at doi:10.1016/j.ejps.2022.106163.

References

Abouir, K., Samer, C.F., Gloor, Y., Desmeules, J.A., Daali, Y., 2021. Reviewing data integrated for PBPK model development to predict metabolic drug-drug interactions: shifting perspectives and emerging trends. Front. Pharmacol. 12, 708299.

Bellanti, F., Della Pasqua, O., 2011. Modelling and simulation as research tools in paediatric drug development. Eur. J. Clin. Pharmacol. 67 (Suppl 1), 75–86.

Bruzzese, T., Rimaroli, C., Bonabello, A., Mozzi, G., Ajay, S., Cooverj, N.D., 2000. Pharmacokinetics and tissue distribution of rifametane, a new 3-azinomethyl-rifamycin derivative, in several animal species. Arzneimittelforschung 50, 60–71.
Carrara, L., Magni, P., Teutonico, D., Pasotti, L., Della Pasqua, O., Kloprogge, F., 2020. Ethambutol disposition in humans: challenges and limitations of whole-body physiologically-based pharmacokinetic modelling in early drug development. Eur. J. Pharm. Sci. 150, 105359.
Conte, J.E., Lin, E., Zurlinden, E., 2000. High-performance liquid chromatographic determination of pyrazinamide in human plasma, bronchoalveolar lavage fluid, and alveolar cells. J. Chromatogr. Sci. 38, 33–37.
Conte, J.E., Golden, J.A., Kipps, J., Lin, E.T., Zurlinden, E., 2001. Effects of AIDS and gender on steady-state plasma and intrapulmonary ethambutol concentrations. Antimicrob. Agents Chemother. 45, 2891–2896.
Conte, J.E., Golden, J.A., McQuitty, M., Kipps, J., Duncan, S., McKenna, E., et al., 2002. Effects of gender, AIDS, and acetylator status on intrapulmonary concentrations of isoniazid. Antimicrob. Agents Chemother. 46, 2358–2364.
Conte, J.E., Golden, J.A., Kipps, J.E., Lin, E.T., Zurlinden, E., 2004. Effect of sex and AIDS status on the plasma and intrapulmonary pharmacokinetics of rifampicin. Clin. Pharmacokinet. 43, 395–404.
Cordes, H., Thiel, C., Aschmann, H.E., Baier, V., Blank, L.M., Kuepfer, L., 2016. A physiologically-based pharmacokinetic model of isoniazid and its application in individualizing tuberculosis chemotherapy. Antimicrob. Agents Chemother. 60, 6134–6145.
Danesi, R., Lupetti, A., Barbara, C., Ghelardi, E., Chella, A., Malizia, T., et al., 2003. Comparative distribution of azithromycin in lung tissue of patients given oral daily doses of 500 and 1000 mg. J. Antimicrob. Chemother. 51, 939–945.
De Buck, S.S., Sinha, V.K., Fenu, L.A., Nijsen, M.J., Mackie, C.E., Gilissen, R.A., 2007. Prediction of human pharmacokinetics using physiologically based modeling: a retrospective analysis of 26 clinically tested drugs. Drug Metab. Dispos. 35, 1766–1780.
Della Pasqua, O., 2013. Translational pharmacology: from animal to man and back. Drug Discov. Today Technol. 10, e315–e317.
DrugBank 2020a. Isoniazid. Retrieved from https://www.drugbank.ca/drugs/DB00951. Accessed June 16, 2020.
DrugBank 2020b. Ethambutol. Retrieved from https://www.drugbank.ca/drugs/DB00330. Accessed June 16, 2020.
DrugBank 2020c. Pyrazinamide. Retrieved from https://www.drugbank.ca/drugs/DB00339. Accessed June 16, 2020.
Gaohua, L., Wedagedera, J., Small, B.G., Almond, L., Romero, K., Hermann, D., et al., 2015. Development of a multicompartment permeability-limited lung PBPK model and its application in predicting pulmonary pharmacokinetics of antituberculosis drugs. CPT Pharmacomet. Syst. Pharmacol. 4, 605–613.
Huang, W., Isoherranen, N., 2020. Sampling site has a critical impact on physiologically based pharmacokinetic modeling. J. Pharmacol. Exp. Ther. 372, 30–45.
Irwin, S.M., Prideaux, B., Lyon, E.R., Zimmerman, M.D., Brooks, E.J., Schrupp, C.A., et al., 2016. Bedaquiline and pyrazinamide treatment responses are affected by pulmonary lesion heterogeneity in Mycobacterium tuberculosis infected C3HeB/FeJ mice. ACS Infect. Dis. 2, 251–267.
Jones, H.M., Parrott, N., Jorga, K., Lav, T., 2006. A novel strategy for physiologically-based predictions of human pharmacokinetics. Clin. Pharmacokinet. 45, 511–542.
Jones, H.M., Mayawala, K., Poulin, P., 2013. Dose selection based on physiologically based pharmacokinetic (PBPK) approaches. AAPS J. 15, 377–387.
Kiem, S., Schentag, J.J., 2008. Interpretation of antibiotic concentration ratios measured in epithelial lining fluid. Antimicrob. Agents Chemother. 52, 24–36.
Kjellsson, M.C., Via, L.E., Goh, A., Weiner, D., Low, K.M., Kern, S., et al., 2012. Pharmacokinetic evaluation of the penetration of antituberculosis agents in rabbit pulmonary lesions. Antimicrob. Agents Chemother. 56, 446–457.
Kuepfer, L., Niederalt, C., Wendl, T., Schlender, J.F., Willmann, S., Lippert, J., et al., 2016. Applied concepts in PBPK modeling: how to build a PBPK/PD model. CPT Pharmacomet. Syst. Pharmacol. 5, 516–531.
Lakshminarayana, S.B., Huat, T.B., Ho, P.C., Manjunatha, U.H., Dartois, V., Dick, T., et al., 2015. Comprehensive physicochemical, pharmacokinetic and activity profiling of anti-TB agents. J. Antimicrob. Chemother. 70, 857–867.
Lee, C.S., Gambertoglio, J.G., Brater, D.C., Benet, L.Z., 1977. Kinetics of oral ethambutol in the normal subject. Clin. Pharmacol. Ther. 22, 615–621.
Lee, C.S., Brater, D.C., Gambertoglio, J.G., Benet, L.Z., 1980. Disposition kinetics of ethambutol in man. J. Pharmacokinet. Biopharm. 8, 335–346.
Lenaerts, A., Barry 3rd, C.E., Dartois, V., 2015. Heterogeneity in tuberculosis pathology, microenvironments and therapeutic responses. Immunol. Rev. 264, 288–307.
Lippert, J., Burghaus, R., Edginton, A., Frechen, S., Karlsson, M., et al., 2019. Open systems pharmacology community-An open access, open source, open science approach to modeling and simulation in pharmaceutical sciences. CPT Pharmacomet. Syst. Pharmacol. 8, 878–882.
Lyons, M.A., Reisfeld, B., Yang, R.S., Lenaerts, A.J., 2013. A physiologically based pharmacokinetic model of rifampin in mice. Antimicrob. Agents Chemother. 57, 1763–1771.
Molina, D.K., DiMaio, V.J., 2012. Normal organ weights in men: part II-the brain, lungs, liver, spleen, and kidneys. Am. J. Forensic Med. Pathol. 33, 368–372.
Muliaditan, M., Della Pasqua, O., 2019. How long will treatment guidelines for TB continue to overlook variability in drug exposure? J. Antimicrob. Chemother. 74, 3274–3280.
Muliaditan, M., Della Pasqua, O., 2021. Bacterial growth dynamics and pharmacokinetic-pharmacodynamic relationships of rifampicin and bedaquiline in BALB/c mice. Br. J. Pharmacol. 179, 1251–1263.
Muliaditan, M., Davies, G.R., Simonsson, U.S.H., Gillespie, S.H., Della Pasqua, O., 2017. The implications of model-informed drug discovery and development for tuberculosis. Drug Discov. Today 22, 481–486.
Nardotto, G.H.B., Bollela, V.R., Rocha, A., Della Pasqua, O., Lanchote, V.L., 2022. No implication of HIV coinfection on the plasma exposure to rifampicin, pyrazinamide, and ethambutol in tuberculosis patients. Clin. Transl. Sci. 15, 514–523.
Poulin, P., Jones, R.D., Jones, H.M., Gibson, C.R., Rowland, M., Chien, J.Y., et al., 2011. PHRMA CPCDC initiative on predictive models of human pharmacokinetics, part 5: prediction of plasma concentration-time profiles in human by using the physiologically-based pharmacokinetic modeling approach. J. Pharm. Sci. 100, 4127–4157.
Prideaux, B., Via, L.E., Zimmerman, M.D., Eum, S., Sarathy, J., O'Brien, P., et al., 2015a. The association between sterilizing activity and drug distribution into tuberculosis lesions. Nat. Med. 21, 1223–1227.
Prideaux, B., Einaggar, M.S., Zimmerman, M., Wiseman, J.M., Li, X., Dartois, V., 2015b. Mass spectrometry imaging of levofloxacin distribution in TB-infected pulmonary lesions by MALDI-MSI and continuous liquid microjunction surface sampling. Int. J. Mass spectrom. 377, 699–708.
R Core Team. R: A language and environment for statistical computing. R foundation for statistical computing, Vienna, Austria. Retrieved from https://www.R-project.org/. Accessed June 16, 2020.
Reisfeld, B., Metzler, C.P., Lyons, M.A., Mayeno, A.N., Brooks, E.J., Degroote, M.A., 2012. A physiologically based pharmacokinetic model for capreomycin. Antimicrob. Agents Chemother. 56, 926–934.
Rohatgi, A. WebPlotDigitizer. Retrieved from https://automeris.io/WebPlotDigitizer. Accessed June 16, 2020.
Romano, F., D'Agate, S., Della Pasqua, O., 2021. Model-informed repurposing of medicines for SARS-CoV-2: extrapolation of antiviral activity and dose rationale for paediatric patients. Pharmaceutics 13, 1299.
Sadiq, M.W., Nielsen, E.I., Khachman, D., Conil, J.M., Georges, B., Houin, G., et al., 2017. A whole-body physiologically based pharmacokinetic (WB-PBPK) model of ciprofloxacin: a step towards predicting bacterial killing at sites of infection. J. Pharmacokinet. Pharmacodyn. 44, 69–79.
Tanaka, G., Kawamura, H. Anatomical and physiological characteristics for Asian reference man: male and female of different ages: tanaka model. Division of Radioecology. National Institute of Radiological Sciences. Hitachinaka 311-12 Japan. Report Number NIRS-M-115 (1996).
TB Alliance, 2008a. Rifampin. Tuberculosis 88, 151–154.
TB Alliance, 2008b. Ethambutol. Tuberculosis 88, 102–105.
Zurlinden, T.J., Eppers, G.J., Reisfeld, B., 2016. Physiologically-based pharmacokinetic model of rifapentine and 25-desacetyl rifapentine disposition in humans. Antimicrob. Agents Chemother. 60, 4860–4868.